



TITLE:

# On the Estimate of the Size and the Optical Anisotropy of Polyethylene Crystals Growing in Dilute Solution

AUTHOR(S):

Suzuki, Hidematsu; Muraoka, Yoichiro

---

CITATION:

Suzuki, Hidematsu ...[et al]. On the Estimate of the Size and the Optical Anisotropy of Polyethylene Crystals Growing in Dilute Solution. Bulletin of the Institute for Chemical Research, Kyoto University 1987, 65(2): 83-95

ISSUE DATE:

1987-07-21

URL:

<http://hdl.handle.net/2433/77186>

RIGHT:

## On the Estimate of the Size and the Optical Anisotropy of Polyethylene Crystals Growing in Dilute Solution

Hidematsu SUZUKI\* and Yoichiro MURAOKA\*\*

*Received April 24, 1987*

A light-scattering method has been derived for estimating the size and the optical anisotropy of large thin discs. An application of the method was made to the data on linear polyethylene isothermally crystallizing in dilute *p*-xylene solution. The results obtained are the variations with time of the following quantities; size, optical anisotropy, mass and concentration of the crystals formed. It became possible to follow the kinetics of the crystal growth directly in situ.

**KEY WORDS:** Light scattering/ Anisotropic thin disc/ Polyethylene/ Crystallization/ Linear growth rate/

### INTRODUCTION

Light scattering appears as the potentially most appropriate method for following the kinetics of crystallization of polymers in dilute solution. This is because the method is so accurate that relatively small quantities and small crystals can give a measurable intensity of scattered light. At the same time, the crystallization itself is by no means interfered with by the measurements. An additional advantage can be found in such a system as polyethylene in *p*-xylene solutions, where the excess scattering intensity over that of the solvent may be considered to be due practically to the crystals because of the negligible difference in refractive index between the solvent and the dissolved polymer. For successful analysis of the experimental data obtained, however, two main problems have to be overcome: the size of crystals formed and their optical anisotropy.

Essentially, the difficulties in these problems come, respectively, from the dimensions of crystals even greater than the wavelength of the light used and from the regular (chain-folded) structure of crystals. To make matters worse, these problems are not independent of each other. In order to meet these difficulties, we will first review the literature methods critically in the following section. Secondly, a novel method for determining the size and the optical anisotropy of crystals at the same time will be presented in the third section, actually being applied to the data on linear polyethylene while crystallizing in dilute *p*-xylene solution. Based on the results obtained, we will discuss the kinetics of crystallization in the fourth section.

---

\*鈴木秀松: Laboratory of Polymer Separation and Characterization, Institute for Chemical Research, Kyoto University, Uji, Kyoto-Fu 611.

\*\*村岡雍一郎: Heian Jogakuin Junior College, Nanpeidai, Takatsuki, Osaka-Fu 569.

## THE LITERATURE METHODS

It would be sensible first to have a close look at typical experimental data as shown in Fig. 1. Here,  $\Delta I(\theta, t)$  is a reading of the intensity of light scattered from crystals at scattering angle  $\theta$  and at measurement time  $t$ . The sample used was NBS SRM 1475 linear polyethylene (the weight-average molecular weight  $M_w = 5.2 \times 10^4$ ), which was isothermally crystallized at  $89.4^\circ\text{C}$  at the initial concentration  $c^0 = 2.24 \times 10^{-4} \text{ g cm}^{-3}$ . The detail of the measurements has been published.<sup>1)</sup> From this figure, several characteristics of the light scattered from polyethylene crystals may be seen. (1) The forward scattering intensity is much stronger than the backward one. This significant degree of interference of scattered lights implies that the scattering particles have dimensions comparable to or even greater than the wavelength of the used light. (2) Accordingly, the usual plot of  $1/\Delta I(\theta, t)$  against  $\sin^2(\theta/2)$ , as shown in panel a of Fig. 1, is apparently unsuccessful in extrapolating the data to  $\theta = 0^\circ$ : the intercept to be obtained is not distinguishable from the origin of the

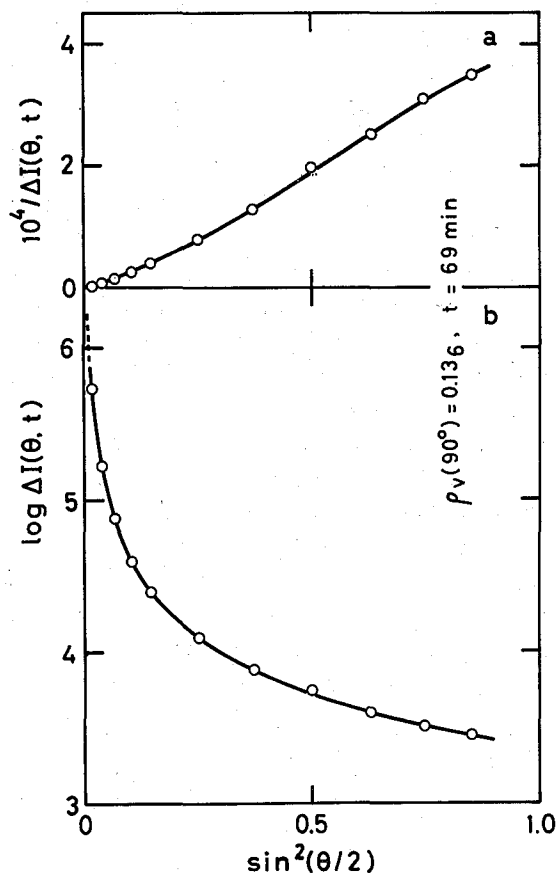


Fig. 1. Angular dependence of the observed intensity of light scattered from polyethylene crystals: (a) usual reciprocal plot and (b) logarithm plot of the same data. See the text for the experimental conditions.

coordinates. (3) The depolarization ratio  $\rho_V(90^\circ)$  evaluated at  $\theta=90^\circ$  was 0.13, for the crystals at this measurement time. Since this large value of  $\rho_V(90^\circ)$  suggests the large optical anisotropy  $\delta$  of the crystals, the anisotropy effects must be taken into account for an accurate estimate of the size of crystals. And (4) the features of the whole scattering envelope are quite different from those of coils, rods, and spheres, but qualitatively similar to that of thin discs, as have already been recognized by several authors.<sup>1-3)</sup>

Figure 2a and 2b are given to show, in another way, the validity of the thin disc approximation to polyethylene crystals growing in dilute solutions. These figures are plots of the experimental ratio  $P(15^\circ)/P(\theta) (\equiv \Delta I(15^\circ)/\Delta I(\theta))$  of the particle scattering factor  $P(\theta)$  against  $t$  in Fig. 2a and its theoretical ratio against  $\log(D/\lambda)$  in Fig. 2b. For this illustration,  $P(\theta)$  for isotropic thin discs<sup>4)</sup>

$$P(\theta) = (2/x^2)[1 - J_1(2x)/x] \quad (1)$$

with  $x = (2\pi D/\lambda) \sin(\theta/2)$  was numerically calculated by use of a FACOM M-160AD digital computer (Fujitsu Ltd., Tokyo) of the Computer Center of this Institute. Here,  $D$  and  $\lambda$  are, respectively, the diameter and the wavelength of the light in the medium and  $J_1$  is the Bessel function of first order. Little is known about the correlation between  $t$  and  $D/\lambda$  except that crystals grow with the passage of time. Nevertheless, mutual characteristics of the ratio  $P(15^\circ)/P(\theta)$  can be seen in these figures. And as a next step, an introduction of the (finite) optical anisotropy will substantiate the validity of the thin disc approximation.

Now the problem is how to estimate the size of the crystals in the disc approximation. Scholte<sup>2)</sup> simply abandoned the extrapolation and the size determination: instead he evaluated crystal concentrations from the intensities of scattered lights in the approximation of optically isotropic thin discs. In his analysis, a single experimental datum of  $\Delta I(30^\circ)$  was used as the reference instead of that extrapolated to zero scattering angle. The reference like this might be subject to larger error. Picot et al.<sup>3)</sup> extrapolated the scattered-light intensity on a plot like Fig. 1b. Such an extrapolation seems to be natural, since the linear portion of the  $P(\theta)$  curve is retained on the plot over the range of scattering angles accessible experimentally. Figure 3a shows two examples for discs with an equal size of  $D/\lambda = 2.0$  but with different optical anisotropies of  $\delta = 0$  and 0.4. The  $P(\theta)$  for anisotropic thin discs, which will be given below, has been numerically calculated just as for isotropic ones and illustrated on this figure for the aforementioned case. On plots of this type, Picot et al. determined the initial slope of the  $P(\theta)$  curve to estimate the mean-square radius of gyration  $\langle s^2 \rangle$  of crystals, which was converted later into the diameter by use of the relation  $\langle s^2 \rangle = D^2/8$  for thin discs. Those evaluations were carried out without any correction to the estimated initial slope for anisotropy effects. This procedure has two shortcomings. First, as is obvious in Fig. 3a, the initial slope varies with the  $\delta$  value even if the size of a disc is fixed. The isotropic disc approximation cannot be valid to estimate the diameter of an anisotropic disc. The second shortcoming is seen from Fig. 3b. Such an extrapolation is no longer possible for discs with the size larger than  $D/\lambda = 3.0$  so long as the data at scattering angles lower than  $10^\circ$  are not available. The crystal sizes actually encountered during experiments might exceed this limit of the applicability. Therefore, it is highly likely that the size of the crystal has been underestimated to some extent in the analysis of Picot et al.

The method adopted in our previous paper<sup>1)</sup> is based on the extrapolation as made by

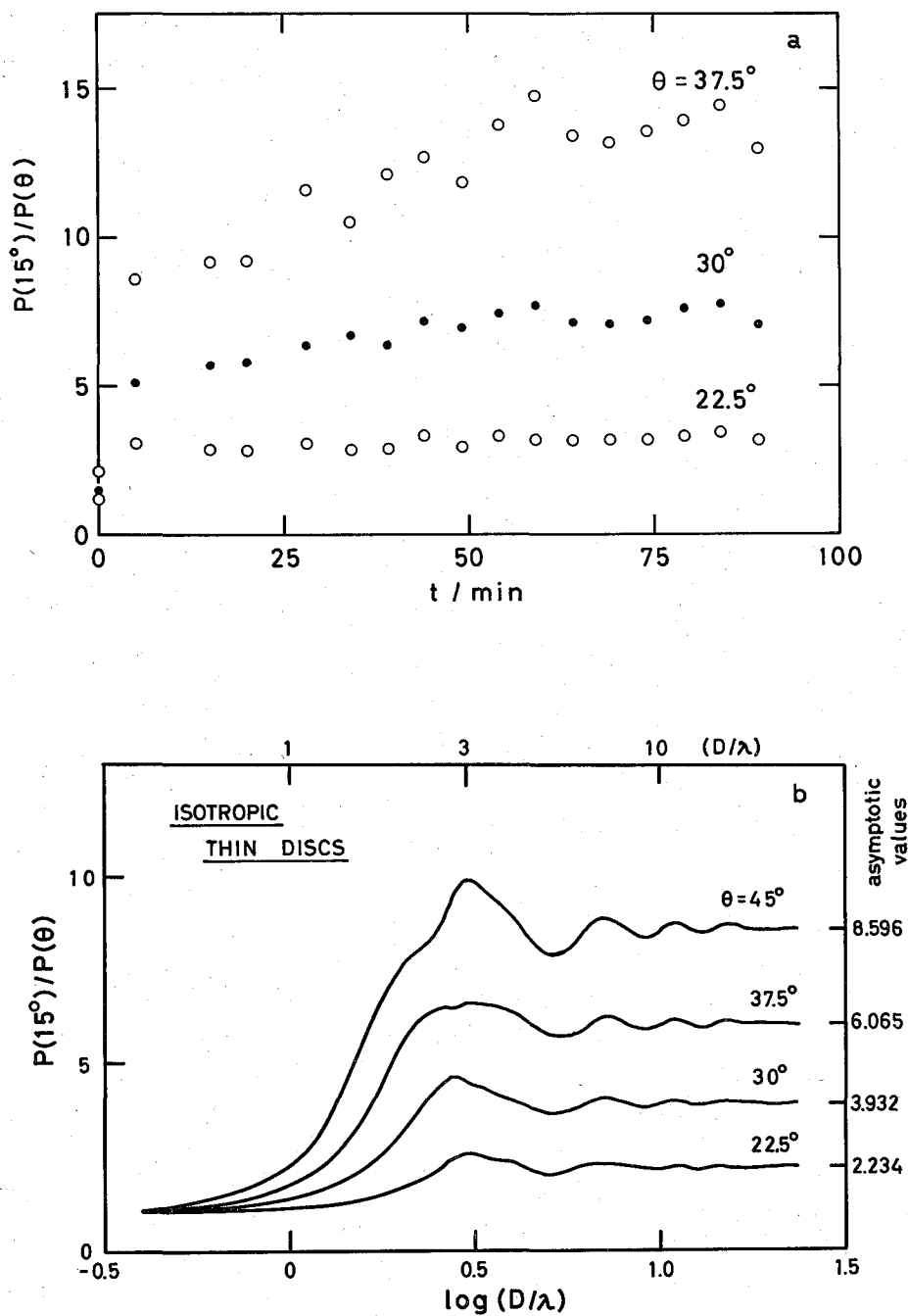


Fig. 2. (a) Variation of the experimental ratio  $P(15^\circ)/P(\theta)$  with  $t$  at three lower scattering angles. (b) Variation of its theoretical ratio with  $\log(D/\lambda)$  for isotropic thin discs.

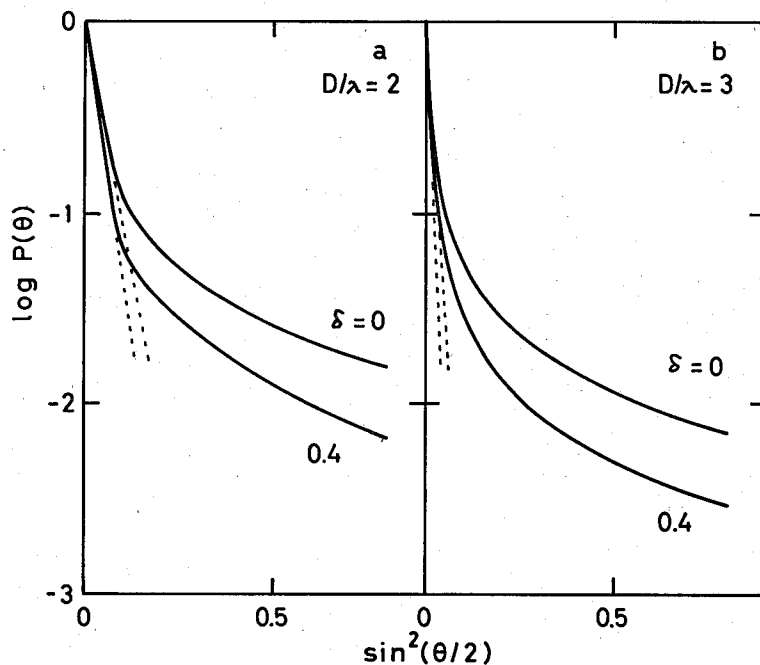


Fig. 3. Theoretical dependence of  $\log P(\theta)$  on  $\sin^2(\theta/2)$  for discs with  $D/\lambda$  of 2 (a) and 3 (b).

Picot et al., but the initial slope was not used for estimating the size. The experimental  $P(\theta)$  values as calculated by  $\Delta I(\theta)/\Delta I(0^\circ)$  were compared with the theoretical ones for a disc with a given value of  $D/\lambda$ . The  $D/\lambda$  value was sought to give the best fit between the experimental and theoretical  $P(\theta)$  values. It has been seen that an introduction of the optical anisotropy improves such fittings.<sup>1)</sup> The degree of the optical anisotropy had been determined separately. However, this method cannot also be free from the second shortcoming mentioned above, for the same type of extrapolation is essential to calculate the experimental  $P(\theta)$  values.

The optical anisotropy of larger particles is generally difficult to be determined. Picot et al.<sup>3)</sup> measured the anisotropic component of scattered light over the  $\theta$ -range as wide as for the isotropic component and determined the depolarization ratio  $\rho_V(\theta=0^\circ)$  with extrapolated isotropic and anisotropic components of the scattered lights. Theoretically, this is a standard method for determining the optical anisotropy, because the relation

$$\rho_V(0^\circ) = 3\delta^2 / (5 + 4\delta^2) \quad (2)$$

holds irrespective of the size and shape of scattering particles. In practice, however, measurements of the anisotropic component cannot be so accurate as that of the isotropic one except at scattering angles around  $90^\circ$ . Accordingly, another method was proposed in our previous paper.

This is based on the relation :

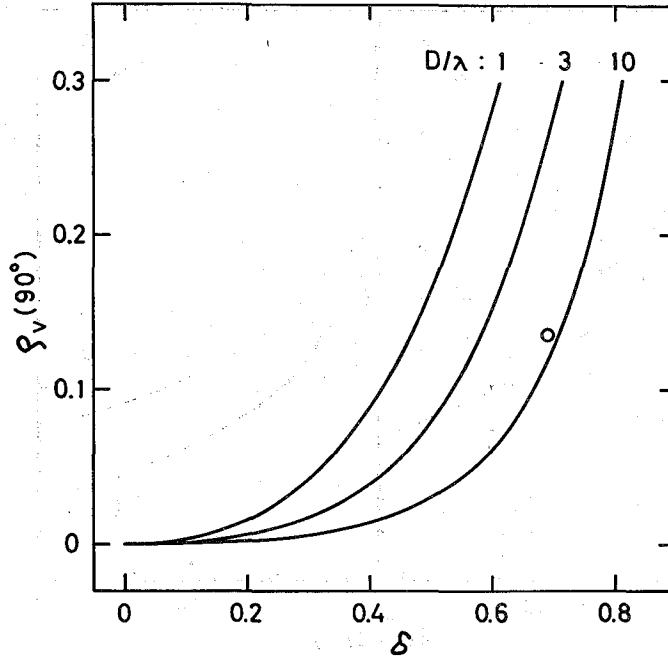


Fig. 4. Theoretical curves of  $\rho_v(90^\circ)$  vs.  $\delta$  for anisotropic thin discs with different sizes. Open circle is the experimental point, as specified by  $(\rho_v(90^\circ), D/\lambda) = (0.13, 7.8)$ , from which  $\delta$  is read as 0.68.

$$\rho_v(90^\circ) = \rho_v(0^\circ) Q[\delta, P(90^\circ)] \quad (3)$$

where  $Q[\delta, P(90^\circ)]$  is a factor taking account of the effects of  $\delta$  and the intramolecular interference, and  $P(90^\circ)$  value observed for anisotropic particles by use of vertically polarized lights  $V_v$ . Since the size and shape of the anisotropic particles of our interest are already known, the plots of  $\rho_v(90^\circ)$  against  $\delta$ , as in Fig. 4, may be used as charts for estimating the  $\delta$  value for the crystal with a known value of  $D/\lambda$ .

It can be said that this method is valid only for the cases where size estimates are reasonably certain. For other cases like the discs with the  $D/\lambda$  values larger than 3.0, the  $\delta$  value estimated might be as ambiguous as the  $D/\lambda$  value is. Hence, a new method is desired in which both  $D/\lambda$  and  $\delta$  are determined more reasonably and unambiguously.

#### A NOVEL METHOD AND ITS APPLICATION

The particle scattering factor for anisotropic thin discs as observed by use of vertically polarized lights  $V_v$  is expressed by

$$P(\theta) = (2/x^2) \left[ I_1 + \delta(3I_2 - 2I_1) + \delta^2 \left( I_1 - 3I_2 + \frac{27}{8}I_3 \right) \right] \quad (4)$$

with

$$I_1 = 1 - J_1(2x)/x \quad (5a)$$

$$I_2 = \int_0^\pi J_1^2(x \sin \gamma) \sin \gamma d\gamma \quad (5b)$$

and

$$I_3 = \int_0^\pi J_1^2(x \sin \gamma) \sin^3 \gamma d\gamma \quad (5c)$$

where  $\gamma$  is the angle between the axis of the disc and the scattering vector. The  $P(\theta)$  factor was numerically calculated for a given set of the  $D/\lambda$  and  $\delta$  values at the scattering angles used in the measurements, which were, in this case,  $15^\circ, 22.5^\circ, 30^\circ, 37.5^\circ, 45^\circ, 60^\circ, 75^\circ, 90^\circ, 105^\circ$ , and  $120^\circ$ . These theoretical values of  $\log P(\theta)$  are plotted against  $\sin^2(\theta/2) - \delta$  for discs with a fixed size but for different values of  $\delta$ , the  $P(\theta)$  curve being drawn for each  $\delta$  value. Then the points, at a given scattering angle, on these  $P(\theta)$  curves are connected to each other, a curvilinear net like the Zimm plot being constructed. An example is depicted in Fig. 5 for discs with  $D/\lambda = 7.8$ . Such figures for various  $D/\lambda$  values have been prepared for later use.

On the other hand, the experimental particle scattering factor  $P(\theta)_{\text{exptl}}$  remains unknown so long as the extrapolation of  $\Delta I(\theta)$  to zero scattering angle is not carried out successfully. By definition, however, the logarithm of  $P(\theta)_{\text{exptl}}$  is directly proportional to that of the intensity observed :

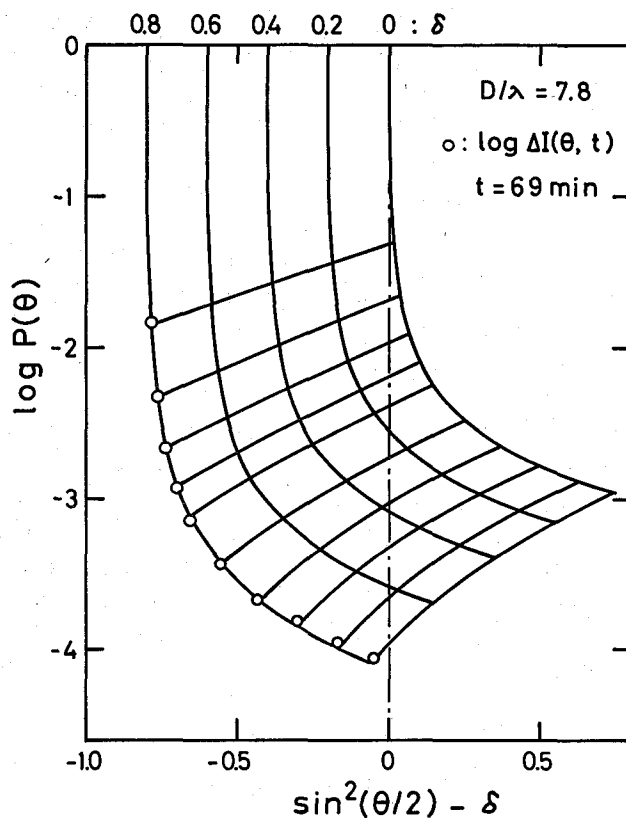


Fig. 5. Superposition of experimental plots of  $\log \Delta I(\theta, t)$  against  $t$  on theoretical plots of  $\log P(\theta)$  against  $\sin^2(\theta/2) - \delta$  for anisotropic thin discs with size of  $D/\lambda = 7.8$ .



Table 1. Results of the estimated size, optical anisotropy and scattered-light intensity at zero scattering angle

$t/\text{min}$	$D/\lambda$	$\delta$	$\log \Delta I(0^\circ)$	$\rho_V(90^\circ)$
15	2.5	0.4	3.90	—
20	3.0	0.4	4.40	—
28	3.8	0.6	5.26	—
34	4.2	0.8	5.90	0.06 <sub>6</sub>
39	4.8	0.8	6.25	0.06 <sub>4</sub>
44	5.2	0.8	6.54	0.07 <sub>8</sub>
49	5.8	0.8	6.80	0.08 <sub>2</sub>
54	6.2	0.8	7.02	0.10 <sub>1</sub>
59	6.8	0.8	7.25	0.10 <sub>9</sub>
64	7.2	0.8	7.36	0.12 <sub>4</sub>
69	7.8	0.8	7.54	0.13 <sub>8</sub>

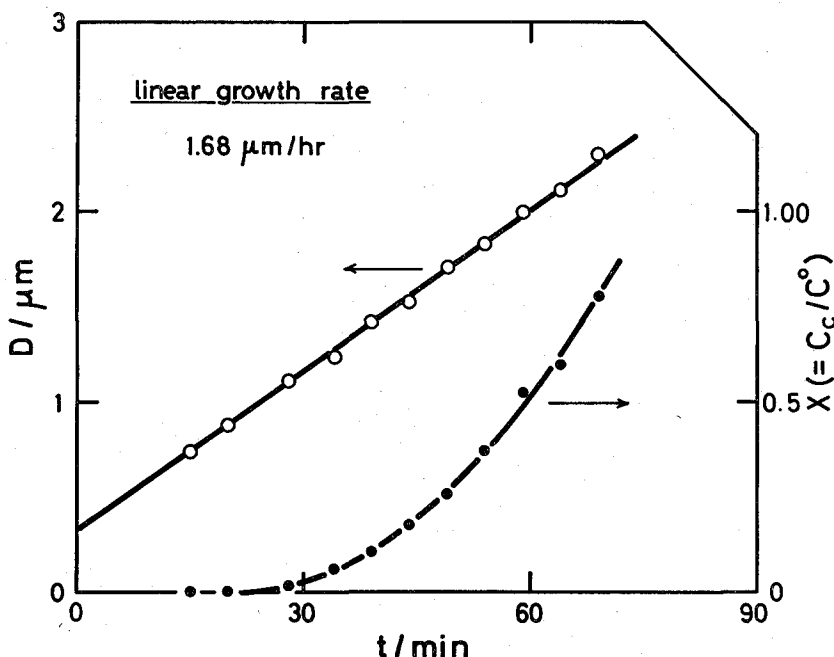
$$\log P(\theta)_{\text{exptl}} = \log \Delta I(\theta) - \log \Delta I(0^\circ) \quad (6)$$

Therefore, a plot of  $\log \Delta I(\theta)$  against  $\sin^2(\theta/2)$  is to be superposed on a theoretical plot like Fig. 5 in order to look for the best fits between the knots of the netlike chart and the points of experimental data. In Fig. 5, an example of the superposition is shown by use of the data presented in Fig. 1: a set of values  $(D/\lambda, \delta) = (7.8, 0.8)$  is found to give the best fit.

In this way of determining the values of  $D/\lambda$  and  $\delta$ , no direct extrapolation of  $\log \Delta I(\theta)$  is necessary,  $\log \Delta I(0^\circ)$  being read as, in the present case, 7.54 from the shift factor according to eq. (6). It should be noted that a reading at the lowest scattering angle  $\Delta I(15^\circ)$  is only as low as 2% of the  $\Delta I(0^\circ)$  value thus determined. Without help of the theoretical charts like Fig. 5,  $\Delta I(0^\circ)$  could not be estimated because of the long extrapolation. This superposition method was applied to all the experimental data. For the data at  $t = 15$  min, the direct extrapolation method was also used, and both methods were found to give the same value of  $\log \Delta I(0^\circ)$ . On the other hand, four sets of the data at  $t = 74-89$  min could not be analyzed even by the present method: the fittings became poor especially at higher scattering angles due probably to the heterogeneity of crystal size. All the results successfully obtained for  $D/\lambda$ ,  $\delta$ , and  $\log \Delta I(0^\circ)$  are summarized in Table 1. In the last column of this table are reproduced the  $\rho_V(90^\circ)$  values previously determined for growing crystals from anisotropic component measurements. This table clearly shows the variation of the  $D/\lambda$  value with time, which was hardly detected in the previous analysis owing to the limited applicability of the method employed. Obviously, this reflects the growth of crystals in solution. The increase in  $\Delta I(0^\circ)$  with time also implies both the increase in crystal mass and the increase in crystal concentration.

### KINETICS OF CRYSTALLIZATION

Now we consider the kinetics of crystallization. Since the wavelength of the used blue light in *p*-xylene is 295 nm, the  $D/\lambda$  values obtained are converted into the bare  $D$  values. Those are plotted against  $t$  in Fig. 6. When the size of crystals is measured by the diameter


 Fig. 6. Plots of  $D$  and  $X (=c/c^{\circ})$  against  $t$ .

in the disc approximation, the linear growth rate  $G$  can be estimated, from the slope of this plot, to be  $1.68 \mu\text{m hr}^{-1}$  at the present experimental conditions. This result is compared with those due to Cooper and Manley<sup>5)</sup> on linear polyethylene ( $M_w = 6.16 \times 10^4$  and  $c^{\circ} = 0.023\text{wt } \%$ ) at different temperatures:  $(G/\mu\text{m hr}^{-1}, T/^{\circ}\text{C}) = (0.46, 90.70), (0.88, 89.80), (3.00, 87.90)$ , and  $(5.20, 86.60)$ .

The scattered-light intensity at zero scattering angle can be expressed by

$$\Delta I(0^{\circ}) = \frac{4\pi^2}{\lambda_0^4 N_A} \frac{I_B}{R_B} n_B^2 \left( \frac{n_c - n_0}{\rho_c} \right)^2 M c_c \quad (7)$$

where  $\lambda_0$  is the wavelength of the used light in vacuo (436 nm);  $N_A$  is Avogadro's number;  $I_B$  is the reading of the intensity of the light scattered by pure benzene at  $\theta = 90^{\circ}$  (932.6);  $R_B$  is the Rayleigh ratio for benzene ( $51.6 \times 10^{-6} \text{ cm}^{-1}$  for the vertical components of the light used and at  $25^{\circ}\text{C}$ );  $n_B$ ,  $n_c$  and  $n_0$  are, respectively, the refractive indexes of benzene, the crystals, and  $p$ -xylene;  $\rho_c$  is the crystal density;  $M$  is the mass of the crystals; and  $c_c$  is the crystal concentration. Using the literature values,  $n_c = 1.557$ ,<sup>6)</sup>  $n_B = 1.519$ , and  $n_0 = 1.473$ ,<sup>3,</sup> and  $\rho_c = 0.9 \text{ g cm}^{-3}$ , we obtain the value of the optical constant in front of the product of  $M c_c$ : that is  $5.87_0$  in this measurement. On the other hand, the mass of the crystals may be calculated from the equation,

$$M = (\pi/4) d D^2 \rho_c N_A \quad (8)$$

in our disc approximation and is listed in Table 2. Here,  $d$  is the thickness of the disc. We know, from the literature,<sup>7,8)</sup>  $d = 15 \text{ nm}$  at our crystallization temperature. The thickness is

Table 2. Results of the estimated crystal mass, crystal concentration, and crystal conversion.

$t/\text{min}$	$10^{-9}M$	$C_c$	$10^2X$
15	3.5	$3.9 \times 10^{-7}$	0.17
20	5.0	$8.6 \times 10^{-7}$	0.38
28	8.0	$3.9 \times 10^{-6}$	1.7
34	9.8	$1.3_8 \times 10^{-5}$	6.2
39	12.8	$2.3_7 \times 10^{-5}$	10.6
44	15.0	$3.9_4 \times 10^{-5}$	17.6
49	18.7	$5.7_5 \times 10^{-5}$	25.7
54	21.4	$8.3_6 \times 10^{-5}$	37.3
59	25.7	$1.1_8 \times 10^{-4}$	52.7
64	28.8	$1.3_5 \times 10^{-4}$	60.3
69	33.8	$1.7_5 \times 10^{-4}$	78.1

some hundred times less than the diameter: as has been assumed hitherto, the discs are certainly thin. Now the crystal concentration is ready to be estimated from the results of  $\Delta I(0^\circ)$  and  $D$ , listed in column 3 of Table 2. The crystal conversion  $X$  as defined by  $c_c/c^\circ$  is plotted against  $t$  in the same figure as the plot of  $D$  against  $t$ . From this figure, the linear growth rate is seen to stay constant up to the conversion of some 80 %. This finding is consistent with that of Holland and Lindenmeyer.<sup>7)</sup>

## DISCUSSION

The principle of the present superposition method for determining the size and the optical anisotropy may be useful for scattering particles of any shape. For anisotropic thin discs, this method has been successfully employed over the range of  $D/\lambda$  where the previous extrapolation method gives only poor results. Now we consider the applicability limit of this method. The criteria used for the goodness of fit between experimental data and theoretical predictions were the shape of the scattering envelope as a whole and each interval between  $\log P(\theta)$  (or  $\log \Delta I(\theta)$ ) values at two successive scattering angles. When these criteria scarcely work for two theoretical plots of  $\log P(\theta)$  against  $\sin^2(\theta/2)$ , it can be said that the sizes of the discs for which the theoretical plots are compared are over the applicability limit. Such an example is shown in Fig. 7 for the case of  $\delta=0.8$ . For easy comparison, the  $\log P(\theta)$  values at the scattering angles used for measurements are shown by open circles. Moreover, a curve is shifted to the other in such a way that the  $\log P(15^\circ)$  values of both curves are at the same height on the figure. Despite a big difference in size of the discs,  $D/\lambda=10$  and 15, it is almost impossible to see any clear difference in the points mentioned above. So we may say the practical limit of the applicability is around 10. This limit of  $D/\lambda=10$  also can be seen for cases of other  $\delta$  values.

The accuracy with which the  $\delta$  value is estimated by this method is some  $\pm 0.1$ , more than two significant figures being inaccessible. The previous method by use of Fig. 4 or more suitably theoretical curves of  $\rho_V(90^\circ)$  vs.  $D/\lambda$  with parameter of  $\delta$  might allow us to get more significant figures for  $\delta$ . For the experimental data shown in Fig. 5, the point,  $(\rho_V(90^\circ),$

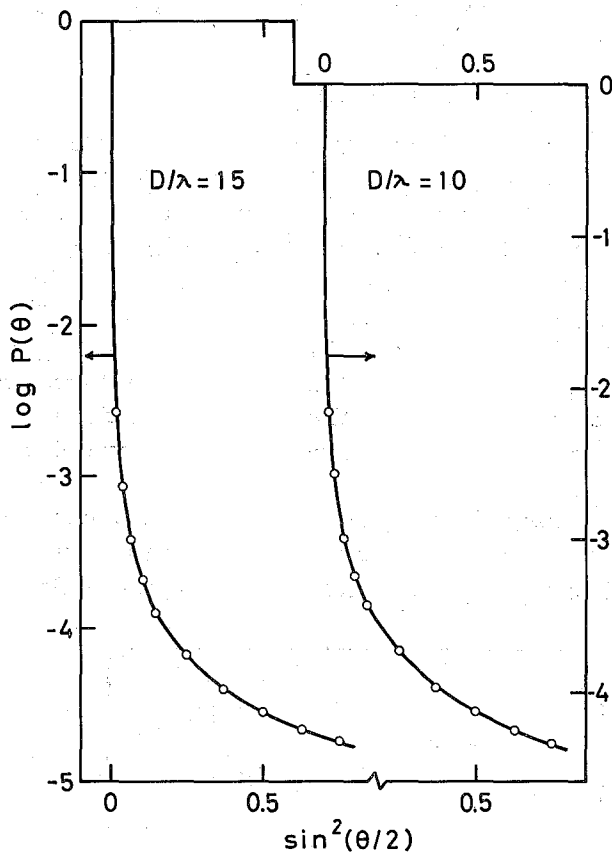


Fig. 7. Comparison of theoretical  $P(\theta)$  curves for anisotropic ( $\delta=0.8$ ) thin discs with different sizes,  $D/\lambda=10$  and 15.

$D/\lambda=(0.13, 7.8)$  can be plotted on Fig. 4 as an open circle, and the  $\delta$  value is read to be 0.68. This result may be more accurate than  $\delta=0.8$  as estimated on Fig. 5. Such refinements of the  $\delta$  values are not made for the other data, however, for we are satisfied with the results obtained by this superposition method.

This crystallization experiment was carried out on a quiescent solution. This is because stirring may change the morphology of the obtained crystals from single crystalline to fibrillar,<sup>9a)</sup> which is not desirable for our purpose. The single crystals grown are, however, not necessarily dispersed homogeneously over the whole solution: it is often seen at the end of measurement that the crystals form large cloudlike clusters. Accordingly, the estimated crystal concentration can only mean its local concentration in the small scattering volume illuminated by the light. That might be quite low or well above the initial concentration, depending on the position of large clusters of the crystals. The estimated value,  $X=78.1\%$  at  $t=69$  min does not necessarily mean close to exhaustion of the polymer in solution. This could be why the linear growth rate stays constant with time throughout the measurement time analyzed.

Most widely, the kinetics of overall crystallization is described by the Avrami-Evans equation.<sup>9b)</sup>

$$X = 1 - \exp(-Kt_c^n) \quad (9)$$

where  $K$  is the rate constant;  $t_c$  is the crystallization time; and  $n$  is the Avrami exponent. The Avrami exponent may show values ranging from below 1 to far above 6, depending on the types of crystallization and nucleation. The present crystallization data are analyzed by this equation in Fig. 8 as a plot of  $\log [-\ln(1-X)]$  against  $\log t_c$ . Here,  $t_c = t - \tau$ : the measurement time is corrected by the estimated delay time of  $\tau = 15$  min. This is a time lag necessary for nucleus formation. From the slope of this plot, we obtain 3.0 for the Avrami exponent and  $3.4 \times 10^{-6}$  for the rate constant. Since the crystals formed approximate discs, we may conclude that the Avrami exponent of 3 expected for thermal nucleation is confirmed. Without the correction of a delay time of 15 min, we found  $n$  to be 4.3 instead of 3.0. This value for  $n$  must be incorrect, changed by the strong correlation between  $K$ ,  $t_c$  and  $n$ .

In conclusion, the superposition method described above allowed us to analyze successfully the light-scattering data on linear polyethylene while isothermally crystallizing in dilute *p*-xylene solution and to follow the kinetics of the crystal growth directly in situ.

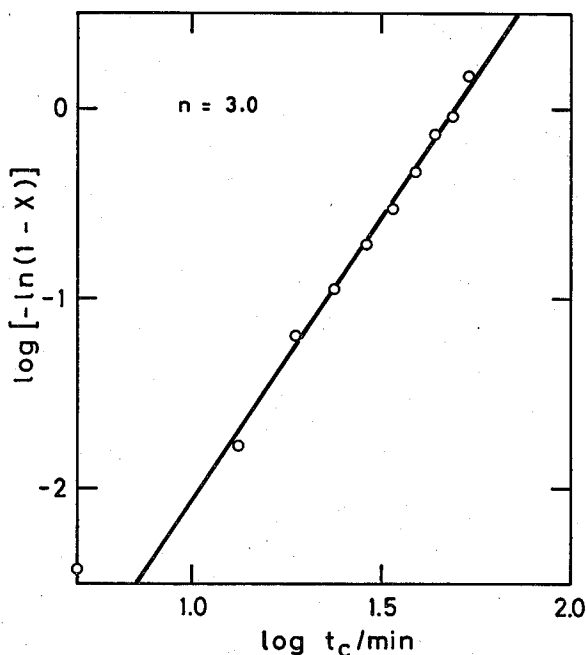


Fig. 8. Analysis of the crystallization results by the Avrami-Evans equation;  $t_c = t - 15$  min

REFERENCES

- (1) H. Suzuki, Y. Muraoka, and K. Kajiura, *Eur. Polym. J.*, **17**, 491 (1981).
- (2) Th. G. Scholte, *J. Polym. Sci. C*, **16**, 1751 (1967).
- (3) C. Picot, G. Weill, and H. Benoit, *J. Colloid Interface Sci.*, **27**, 360 (1968).
- (4) O. Kratky and G. Polod, *J. Colloid Sci.*, **4**, 35 (1945).
- (5) M. Cooper and R. J. Manley, *Macromolecules*, **8**, 219 (1975).
- (6) D. R. Holmes and R. P. Palmer, *J. Polym. Sci.*, **31**, 345 (1958).
- (7) V. F. Holland and P. H. Lindenmeyer, *ibid.*, **57**, 589 (1962).
- (8) A. Nakajima, F. Hamada, S. Hayashi, and T. Sumida, *Kolloid-z. Z. Polym.*, **222**, 10 (1968).
- (9) B. Wunderlich, "Macromolecular Physics", Vol. 2, Academic Press, New York, 1976. (a) p. 207; (b) p. 132.